First-principles study of polarization in $Zn_{1-x}Mg_xO$

Andrei Malashevich* and David Vanderbilt†
Department of Physics & Astronomy, Rutgers University, Piscataway, NJ 08854-8019, USA
(Dated: August 28, 2006)

Wurtzite ZnO can be substituted with up to ∼30% MgO to form a metastable $Zn_{1-x}Mg_xO$ alloy while still retaining the wurtzite structure. Because this alloy has a larger band gap than pure ZnO, $Zn_{1-x}Mg_xO$/ZnO quantum wells and superlattices are of interest as candidates for applications in optoelectronic and electronic devices. Here, we report the results of an *ab-initio* study of the spontaneous polarization of $Zn_{1-x}Mg_xO$ alloys as a function of their composition. We perform calculations of the crystal structure based on density-functional theory in the local-density approximation, and the polarization is calculated using the Berry-phase approach. We decompose the changes in polarization into purely electronic, lattice-displacement mediated, and strain mediated components, and quantify the relative importance of these contributions. We consider both free-stress and epitaxial-strain elastic boundary conditions, and show that our results can be fairly well reproduced by a simple model in which the piezoelectric response of pure ZnO is used to estimate the polarization change of the $Zn_{1-x}Mg_xO$ alloy induced by epitaxial strain.

PACS numbers: 77.22.Ej, 77.65.Bn, 77.84.Bw

I. INTRODUCTION

Recently, much attention has been paid to wurtzite $Zn_{1-x}Mg_xO$ alloys as candidates for applications in optoelectronic devices in the blue and ultraviolet region. ZnO is a wide-band-gap semiconductor with a direct gap of ∼3.3 eV. The band gap becomes even larger if Zn atoms are substituted by Mg atoms, which have a similar ionic radius, allowing the construction of quantum-well and superlattice devices.[1] Similar behavior is well known for the zincblende $GaAs/Al_xGa_{1-x}As$ system and is the basis of much of modern optoelectronics.[2] Recent trends have led in the direction of fabricating similar structures in wide-gap semiconductor systems such as wurtzite III-V nitrides[3] and in $Zn_{1-x}Mg_xO$.[1,4,5] There has also been recent interest in other kinds of nanostructures based on the ZnO and $Zn_{1-x}Mg_xO$ materials systems.[6,7,8,9]

Pure ZnO prefers the wurtzite crystal structure, while MgO adopts the cubic rocksalt structure. Substitution of Zn by Mg results in a metastable wurtzite alloy for certain magnesium concentrations. Experimental reports concerning the growth of these alloys on sapphire substrates indicate that Mg concentrations up to ∼30%,[1,5] or even ∼50%,[10] can be achieved.

Many *ab-initio* calculations of the properties of the parent compounds MgO and ZnO have appeared in the literature.[11,12,13,14] The properties of ternary $Zn_{1-x}Mg_xO$ alloys have been less well studied. There have been calculations of the dependence of the band structure and band gap on concentration x.[15] Regarding the question of crystal structure and stability, Kim *et al.* has shown that the wurtzite $Zn_{1-x}Mg_xO$ alloy is stable with respect to the corresponding rocksalt alloy for $x < 0.375$.[16] Similar results were obtained by Sanati *et al.* but for $x < 0.33$.[17] However, Sanati *et al.* also have shown that $Zn_{1-x}Mg_xO$ is unstable with respect to phase separation into wurtzite ZnO and rocksalt MgO phases even for low x values. This means that $Zn_{1-x}Mg_xO$ alloys are not thermodynamically stable, consistent with a rather low observed solid solubility limit for Mg in ZnO.[18] The success in fabricating samples with higher concentrations indicates that the phase separation is kinetically limited, i.e., the time scale required for the alloy to phase segregate into the two lower-energy constituents is long compared to the growth time at the growth temperature.

To our knowledge, there have not been any previous calculations of the the polarization properties in the $Zn_{1-x}Mg_xO$ system. This is an important property to study, since if an interface occurs between a ZnO region and a $Zn_{1-x}Mg_xO$ region within a superlattice or quantum-well structure, bound charges are expected to appear at the interface. These charges, in turn, will create electric fields that are likely to affect the electrical and optical properties of the quantum-well devices. In the present work, therefore, we have undertaken a study of the polarization and piezoelectric properties of $Zn_{1-x}Mg_xO$.

The structure of the paper is as follows. In the next section we describe the computational methods used in our work. In Sec. III we introduce the six supercell structures that were constructed and used as the structural models for the alloys of interest. Then, in Sec. IV, we report the main results of this work. Finally, a brief summary is given in Sec. V.

II. COMPUTATIONAL METHODS

Calculations of structural and polarization properties are carried out using a plane-wave pseudopotential approach to density-functional theory (DFT). We use the ABINIT code package[19] with the local-density approximation (LDA) implemented using the Teter parametrization of the exchange-correlation[20] and with Troullier-Martins pseudopotentials.[21] For the Zn pseudopotential the $3d$ valence electrons are included in the valence, as

their presence has a significant effect on the accuracy of results.[22] A plane-wave basis set with an energy cutoff of 120 Ry is used to expand the electronic wave functions. A $6 \times 6 \times 4$ Brillouin-zone k-point sampling is used for pure wurtzite ZnO, and equivalent k-point meshes are constructed for use in all wurtzite supercell calculations. The electric polarization is calculated using the Berry-phase approach.[23]

III. SUPERCELL STRUCTURES

In the present work we study the properties of six different models of the ternary $Zn_{1-x}Mg_xO$ alloy, to be described shortly. However, first consider pure wurtzite ZnO. It can be viewed as two identical hexagonal closed-packed (*hcp*) lattices; we take the O sublattice to be shifted in the $+\hat{z}$ direction relative to the Zn sublattice. Three parameters determine this structure: a and c are the lattice constants of the *hcp* lattice, and u describes the shift between the two sublattices.

Replacing some of the Zn atoms by Mg atoms, we get a ternary $Zn_{1-x}Mg_xO$ alloy. Of course, the real alloy is highly disordered. In order to carry out calculations using periodic boundary conditions, we construct ordered supercells having the same Mg concentration x as the alloy of interest. By comparing properties of different supercells having the same x, we may obtain a rough estimate of the size of the errors that result from the replacement of the true disordered alloy by an idealized supercell model.

When constructing supercells, we restricted ourselves to structures having hexagonal symmetry about the z-axis, since real $Zn_{1-x}Mg_xO$ alloys have this symmetry on average. This makes the calculation and interpretation of the results easier. We constructed six model alloy structures: one for $x = 1/6$ (Model 1), two for $x = 1/4$ (Models 2 and 3), one for $x = 1/3$ (Model 4) and two for $x = 1/2$ (Models 5 and 6), as follows.

The simplest alloy one can make (Model 5) is obtained by replacing the Zn atoms by Mg atoms in every second Zn layer along z, giving a structure with Mg concentration $x = 1/2$ and retaining the primitive periodicity of pure ZnO (four atoms per cell). Similarly, if one replaces every fourth layer of Zn by Mg, one arrives a model with $x = 1/4$ (Model 2); this has an eight-atom supercell with the primitive 1×1 in-plane periodicity but with a doubled periodicity along the z-direction.

In the remaining models, we retain the primitive periodicity along z but expand the size of the supercell in the x-y plane, as illustrated in Fig. 1. Models having 2×2 in-plane periodicity (Models 3 and 6), and those having $\sqrt{3} \times \sqrt{3}$ periodicity (Models 1 and 4), are specified with reference to Figs. 1(a) and (b), respectively. Models 3 and 6 thus have 16 atoms per supercell, while Models 1 and 4 have 12 atoms. In Model 3 we assign b = c = Zn and a = d = Mg in Fig. 1(a), obtaining a model with $x = 1/4$ in each cation layer and $x = 1/4$ overall. Model 6 corresponds to b = d = Zn and a = c = Mg; this results in alternating cation layers with $x = 1/4$ and $x = 3/4$, for an overall Mg concentration of $x = 1/2$. Turning to the $\sqrt{3} \times \sqrt{3}$ structures in Fig. 1(b), one can see that the hexagonal symmetry requires that all atoms must be the same (c atoms) in one of the layers. We construct Model 1 by assigning b = c = Zn and a = Mg, yielding alternating layers with $x = 0$ and $x = 1/3$ for an average $x = 1/6$. Finally, for Model 4 we set a = c = Zn and b = Mg so that the layer concentrations are $x = 0$ and $x = 2/3$, averaging to $x = 1/3$.

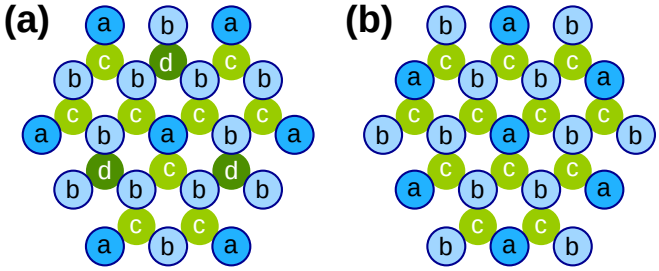

FIG. 1: (Color online.) Top view of cation layers of supercell models for $Zn_{1-x}Mg_xO$ alloys. (a) Structures with 2×2 periodicity (Models 3 and 6). (b) Structures with $\sqrt{3} \times \sqrt{3}$ periodicity (Models 1 and 4). Atoms 'a' and 'b' lie in the top cation layer, while 'c' and 'd' are one layer below (see text).

Of course, it would be possible to generate more supercell models of the alloy by expanding the periodicity or reducing the symmetry. However, the six models described above provide a reasonable coverage of concentrations in the range $0 \leq x \leq 1/2$ with some redundancy (for $x = 1/4$ and $x = 1/2$). We have thus chosen to limit ourselves to these six models in the present work.

IV. RESULTS

A. Pure ZnO and MgO

To determine the crystal structures and cell parameters of pure ZnO and MgO, we carried out DFT calculations for both materials in both the wurtzite and rocksalt structures. For wurtzite ZnO we obtained lattice parameters $a = 3.199$ Å, $c = 5.167$ Å and $u = 0.379$. While these results are very close to previously reported theoretical values,[24] they slightly differ from experimental values[25] ($a = 3.258$ Å, $c = 5.220$ Å and $u = 0.382$). The cohesive energy (defined as the energy per formula unit needed to separate the crystal into atoms) is found to be 8.26 eV. Comparing this to the cohesive energy of rocksalt ZnO (8.03 eV), one may conclude that ZnO prefers the wurtzite structure, in agreement with experiment. For rocksalt MgO we found $a = 4.240$ Å and a cohesive energy of 10.00 eV. We find that if we start with a plausible wurtzite MgO structure with a, c and u similar to that of ZnO, the crystal can monotonically lower

TABLE I: Theoretical equilibrium lattice parameters for bulk ZnO and for models of $Zn_{1-x}Mg_xO$. Subscript 'free' indicates zero-stress elastic boundary conditions, while 'epit' indicates that a is constrained to be identical to that of bulk ZnO (the values in column V are thus identical by construction).

	x	$a_{\rm free}$ (Å)	$(c/a)_{\rm free}$	$a_{\rm epit}$ (Å)	$(c/a)_{\rm epit}$
ZnO	0.0	3.199	1.615	3.199	1.615
Model 1	0.17	3.216	1.605	3.199	1.624
Model 2	0.25	3.230	1.593	3.199	1.625
Model 3	0.25	3.225	1.600	3.199	1.628
Model 4	0.33	3.238	1.589	3.199	1.630
Model 5	0.5	3.266	1.564	3.199	1.635
Model 6	0.5	3.256	1.580	3.199	1.640

its energy along a transformation path in which a increases, c decreases, and u tends toward 1/2 in agreement with the previous results of Ref. 13. The minimum occurs at $u = 1/2$, which corresponds to the higher-symmetry h-MgO structure.[13] For this structure we obtain $a = 3.527\,$Å and $c = 4.213\,$Å, in good agreement[11,13] with previous calculations. We find its cohesive energy to be 9.81 eV, consistent with the fact that MgO prefers the rocksalt structure. (For more details concerning the previous theoretical literature on lattice parameters and binding energies, see Ref. 11.)

The main goal of the present work is to study the polarization and piezoelectric properties of $Zn_{1-x}Mg_xO$. For reference, our calculated spontaneous polarization for pure ZnO is found to be $-0.0322\,{\rm C/m^2}$, and its piezoelectric coefficients are $e_{31} = -0.634\,{\rm C/m^2}$ and $e_{33} = 1.271\,{\rm C/m^2}$. Note that the value of the spontaneous polarization differs somewhat from the previous theory of Dal Corso *et al.*,[12] who reported a polarization of $-0.05\,{\rm C/m^2}$ when using the experimental $u = 0.382$; our value becomes much closer to theirs if we also use the experimental u. Since we are primarily interested in *differences* of the polarization with respect to pure ZnO, we do not believe that these small discrepancies are important. The values of piezoelectric coefficients are in good agreement with previous theoretical calculations of Wu *et al.*[26] who found $e_{31} = -0.67\,{\rm C/m^2}$ and $e_{33} = 1.28\,{\rm C/m^2}$ (and who also provide comparisons with other theoretical and experimental results).

B. Crystal structure and energies of alloys

For each model described in Sec. III, we calculated the *hcp* lattice parameters a and c in the equilibrium state. Since we are interested in properties of $Zn_{1-x}Mg_xO$ layers that might be grown on a ZnO substrate, we also calculated the lattice parameters for epitaxially strained structures (i.e., a fixed to that of pure ZnO). The results are given in Table I. In both cases, the c/a ratio exhibits an almost linear dependence on x. However, this ratio is found to decrease with x for the fully relaxed structures, while it increases with x when the epitaxial strain condition is enforced.

TABLE II: Theoretical cohesive and formation energies (eV per formula unit) for bulk ZnO and MgO and for each supercell model.

	x	$E_{\rm coh}$	$E_{\rm form}$
ZnO	0.0	8.258	0.0
Model 1	0.17	8.496	−0.053
Model 2	0.25	8.602	−0.093
Model 3	0.25	8.612	−0.083
Model 4	0.33	8.729	−0.123
Model 5	0.5	8.955	−0.176
Model 6	0.5	8.958	−0.173
MgO	1.0	10.004	0.0

In Table II we give cohesive and formation energies for each alloy. One can see that in every case the formation energy is negative. Thus, according to our LDA calculations, at zero temperature the $Zn_{1-x}Mg_xO$ alloy is never stable with respect to phase-separated wurtzite ZnO and rocksalt MgO. (Of course, at $T > 0$ a small solid solubility of Mg in wurtzite ZnO is expected.[18])

C. Polarization and piezoelectric properties

The results of the calculations of spontaneous polarization are given in Table III, both for the fully relaxed and for the epitaxially strained cases. Note that the values of polarization for models having the same x are fairly consistent with one another; the choice of supercell does not significantly affect the overall trend with x, which is reasonably smooth. A linear fit $P(x) = P({\rm ZnO}) + Ax$ yields coefficients of $A_{\rm free} = (-0.088 \pm 0.009)\,{\rm C/m^2}$ and $A_{\rm epit} = (0.024 \pm 0.002)\,{\rm C/m^2}$. The latter value may be of direct interest for experimental studies of epitaxial superlattices and quantum wells.

Thus, with increasing Mg concentration x, the absolute value of the polarization increases for the relaxed structures and decreases for the epitaxial structures with fixed a. This behavior is very similar to what we saw in Sec. IV B for the c/a ratios, suggesting that the c/a ratio may be a dominant factor in determining the total polarization. Indeed, since $2e_{31} + e_{33} \simeq 0$, one expects the polarization to be almost independent of a change in volume (isotropic strain), so that the change of c/a should be the most important strain effect.

In order to study more thoroughly the role of strain and other factors in determining the polarizations of the $Zn_{1-x}Mg_xO$ structures, we first define $\Delta P_{\rm tot}$ to be the polarization of the alloy superlattice structure relative to that of pure ZnO. We then decompose $\Delta P_{\rm tot}$ into "electronic," "ionic," and "piezoelectric" contributions as follows. First, we construct an artificial $Zn_{1-x}Mg_xO$ superlattice structure in which the structural paramters (a, c, and all internal coordinates) are frozen to be those of pure ZnO, and define $\Delta P_{\rm elec}$ to be the polarization

TABLE III: Calculated values of total polarizations of $Zn_{1-x}Mg_xO$ alloy models (C/m^2). Subscript 'free' indicates zero-stress elastic boundary conditions, while 'epit' indicates that a is constrained to be identical to that of bulk ZnO. Superscript 'est' indicates value estimated by the model of Eq. 1).

	x	$P_{\rm free}$	$P_{\rm epit}$	$P^{\rm est}_{\rm epit}$
ZnO	0.0	−0.0322	−0.0322	
Model 1	0.17	−0.0423	−0.0277	−0.0279
Model 2	0.25	−0.0501	−0.0247	−0.0247
Model 3	0.25	−0.0470	−0.0244	−0.0250
Model 4	0.33	−0.0565	−0.0230	−0.0239
Model 5	0.5	−0.0789	−0.0199	−0.0222
Model 6	0.5	−0.0699	−0.0202	−0.0225

of this structure relative to that of pure ZnO. Next, we allow only the internal coordinates of the $Zn_{1-x}Mg_xO$ supercell to relax, while continuing to keep a and c frozen at the pure-ZnO values, and let $\Delta P_{\rm ion}$ be the polarization change produced by this internal relaxation. Finally, we allow the lattice constants to relax as well, and define $\Delta P_{\rm piezo}$ to be the associated change in polarization. Clearly $\Delta P = \Delta P_{\rm elec} + \Delta P_{\rm ion} + \Delta P_{\rm piezo}$.

The results of such a decomposition are given in Table IV for the stress-free case. For scale, recall that these are changes relative to $P({\rm ZnO}) = -0.0322\,{\rm C/m^2}$. The purely electronic contributions $\Delta P_{\rm elec}$ are quite small, showing a relatively poor correlation with x. The contribution $\Delta P_{\rm ion}$ associated with the ionic relaxations is also quite small, although it is typically 2-3 times larger than $\Delta P_{\rm elec}$ and shows a clearer trend (becoming more negative with increasing x). By far the largest contribution comes from the piezoelectric effect of the strain relaxation, being typically 5-10 times larger than the ionic one. A similar table can be constructed for the case of epitaxial strain; its first four columns would be identical to Table IV because of the way $\Delta P_{\rm ion}$ and $\Delta P_{\rm elec}$ are defined, and the values in the remaining columns can be deduced from the information given in Tables III and IV. The results indicate that the piezoelectric contribution also dominates in the epitaxial-strain case.

This being the case, it seems likely that many of the polarization-related properties of the $Zn_{1-x}Mg_xO$ alloy can be estimated by using a model based on the piezoelectric effect alone. For example, one might hope that $\delta P = P_{\rm epit} - P_{\rm free}$, the difference between the epitaxially-constrained and free-stress polarizations at a given x, could be estimated by a linear approximation of the form

$$\delta P = 2e_{31}\frac{a_{\rm epit} - a_{\rm free}}{a_{\rm free}} + e_{33}\frac{c_{\rm epit} - c_{\rm free}}{c_{\rm free}}. \qquad (1)$$

In fact, we find that this is the case even if we use the piezoelectric constants of bulk ZnO, already obtained in Sec. IV A, in this formula. Using the computed value of $P_{\rm free}$ reported in the third column of Table III, together with the constrained a values and epitaxially-relaxed c values given in the last two columns of Table I, we report the computed estimates $P^{\rm est}_{\rm epit} = P_{\rm free} + \delta P$ in the last column of Table III. The use of the piezoelectric coefficients of pure ZnO is not obviously justified except at small x, but the results show excellent agreement with the computed $P_{\rm epit}$ values in the fourth column even up to $x = 0.5$, where the error is only about 10%. This approximation thus seems to work quite well.

TABLE IV: Theoretical values of electronic, ionic, piezoelectric and total contributions to polarization (C/m^2) for each model, relative to bulk ZnO.

	x	$\Delta P_{\rm elec}$	$\Delta P_{\rm ion}$	$\Delta P_{\rm piezo}$	$\Delta P_{\rm tot}$
ZnO	0.0	0.0	0.0	0.0	0.0
Model 1	0.17	0.0001	−0.0022	−0.0081	−0.0101
Model 2	0.25	0.0018	−0.0023	−0.0175	−0.0180
Model 3	0.25	0.0000	−0.0027	−0.0122	−0.0148
Model 4	0.33	0.0009	−0.0038	−0.0214	−0.0243
Model 5	0.5	0.0023	−0.0063	−0.0427	−0.0467
Model 6	0.5	−0.0019	−0.0062	−0.0296	−0.0377

V. SUMMARY

We have investigated the polarization-related properties of wurtzite $Zn_{1-x}Mg_xO$ alloys using calculations based on density-functional theory in the local-density approximation and the Berry-phase approach to calculating electric polarization. In particular, we have studied the dependence of the spontaneous polarization on Mg concentration using six alloy supercell models with hexagonal symmetry, spanning the range of Mg concentration from $x = 1/6$ to $1/2$. We performed these calculations both for free-stress and epitaxial-strain elastic boundary conditions.

Our results indicate a roughly linear dependence of spontaneous polarization on Mg concentration, although the sign of the linear coefficient is opposite in the free-stress and epitaxial-strain cases. In order to understand this behavior in more detail, we decomposed the change in polarization into electronic, lattice-displacement-mediated, and strain-mediated components, and found that the latter component is dominant. This means that the change in polarization is mostly governed by piezoelectric effects connected with the x-dependent changes of the a and c lattice constants. We further confirmed this picture by showing that the polarization changes could be well approximated by a model in which the only first-principles inputs to the model are the piezoelectric coefficients of pure ZnO and the x-dependence of the equilibrium lattice constants of the $Zn_{1-x}Mg_xO$ alloy. These results suggest that charging effects associated with polarization discontinuities in $ZnO/Zn_{1-x}Mg_xO$ superlattices and quantum wells should be subject to prediction and interpretation in a fairly straightforward manner.

Acknowledgments

This work was supported by NSF Grant DMR-0549198.

---

* Electronic address: andreim@physics.rutgers.edu
† Electronic address: dhv@physics.rutgers.edu

[1] A. Ohtomo, M. Kawasaki, T. Koida, K. Masubuchi, H. Koinuma, Y. Sakurai, Y. Yoshida, T. Yasuda, and Y. Segawa, Appl. Phys. Lett. **72**, 2466 (1998).
[2] S. Adachi, *GaAs and Related Materials* (World Scientific Publishing Co., 1994).
[3] A. Bykhovski, B. Gelmont, M. Shur, and A. Khan, J. Appl. Phys. **77**, 1616 (1995).
[4] T. Gruber, C. Kirchner, R. Kling, F. Reuss, and A. Waag, Appl. Phys. Lett. **84**, 5359 (2004).
[5] X. Zhang, H. Ma, Q. Wang, J. Ma, F. Zong, H. Xiao, and S. H. F. Ji, Physica B **364**, 157 (2005).
[6] Z. C. Tu and X. Hu, Phys. Rev. B **74**, 035434 (2006).
[7] H. J. Xiang, J. Yang, J. G. Hou, and Q. Zhu, cond-mat/0511473.
[8] Y. W. Heo, M. Kaufman, K. Pruessner, D. P. Norton, F. Ren, M. F. Chisholm, and P. H. Fleming, Solid-State Electron. **47**, 2269 (2003).
[9] Y. W. Heo, C. Abernathy, K. Pruessner, W. Sigmund, D. P. Norton, M. Overberg, F. Ren, and M. F. Chisholm, J. Appl. Phys. **96**, 3424 (2004).
[10] N. B. Chen, H. Z. Wu, D. J. Qiu, T. N. Xu, J. Chen, and W. Z. Shen, J. Phys.: Condens. Matter **16**, 2973 (2004).
[11] A. Schleife, F. Fuchs, J. Furthmüller, and F. Bechstedt, Phys. Rev. B **73**, 245212 (2006).
[12] A. D. Corso, M. Posternak, R. Resta, and A. Baldareschi, Phys. Rev. B **50**, 10715 (1994).
[13] S. Limpijumnong and W. R. L. Lambrecht, Phys. Rev. B **63**, 104103 (2001).
[14] P. Gopal and N. A. Spaldin, cond-mat/0507217.
[15] W. R. L. Lambrecht, S. Limpijumnong, and B. Segall (1999), MRS Internet J. Nitride Semicond. Res. 4S1, G6.8.
[16] Y.-S. Kim, E.-C. Lee, and K. J. Chang, Journal of the Korean Physical Society **39**, S92 (2001).
[17] M. Sanati, G. L. W. Hart, and A. Zunger, Phys. Rev. B **68**, 155210 (2003).
[18] J. F. Sarver, F. L. Katnack, and F. A. Hummel, J. Electrochem. Soc. **106**, 960 (1959).
[19] X. Gonze, J. M. Beuken, R. Caracas, F. Detraux, M. Fuchs, G. M. Rignanese, L. Sindic, M. Verstraete, G. Zerah, F. Jollet, et al., Comput. Mater. Sci. **25**, 478 (2002).
[20] S. Goedecker, M. Teter, and J. Huetter, Phys. Rev. B **54**, 1703 (1996).
[21] N. Troullier and J. L. Martins, Phys. Rev. B **43**, 1993 (1991).
[22] N. A. Hill and U. Waghmare, Phys. Rev. B **62**, 8802 (2000).
[23] R. D. King-Smith and D. Vanderbilt, Phys. Rev. B **47**, 1651 (1993).
[24] J. Serrano, A. H. Romero, F. J. Manjón, R. Lauck, M. Cardona, and A. Rubio, Phys. Rev. B **69**, 094306 (2004).
[25] F. Decremps, F. Datchi, A. M. Saitta, A. Polian, S. Pascarelli, A. DiCicco, J. P. Itié, and F. Baudelet, Phys. Rev. B **68**, 104101 (2003).
[26] X. Wu, D. Vanderbilt, and D. R. Hamann, Phys. Rev. B **72**, 035105 (2005).